生物散斑技术在水果品质检测中的应用及图像处理算法进展

邓博涵[1]，陈嘉豪[1]，胡孟晗[2]，许文平[1**]，张才喜[1*]

[1]上海交通大学农业与生物学院，上海 200240；

[2]华东师范大学信息科学技术学院上海市多维度信息处理重点实验室，上海 200241

摘要 生物散斑是一种利用激光在物体内部的折射与反射来反映其内部信息的光学无损检测技术。生物散斑成像设备和图像处理算法不断改进，应用领域也在逐步扩大；但由于干扰因素的存在，建模精度仍是研究者关注的重点。本文较为详尽地整理了散斑图像处理算法，并对生物散斑技术在水果品质检测中的应用进行调研，归纳主要的成像设备，提出改进意见，旨在为后续研究提供启发。

关键词 激光光学；生物散斑；水果品质检测；激光散斑；图像处理算法

中图分类号 O439 **文献标识码** A **doi**：10.3788/LOP56.090003

Application and Imaging Processing Algorithm of Biospeckle Technology in Fruit Quality Detection

Deng Bohan[1], Chen Jiahao[1], Hu Menghan[2], Xu Wenping[1**], Zhang Caixi[1*]

[1] *School of Agriculture and Biology, Shanghai Jiao Tong University, Shanghai* 200240, *China*;

[2] *Shanghai Key Laboratory of Multidimensional Information Processing, School of Information Science Technology, East China Normal University, Shanghai* 200241, *China*

Abstract Biospeckle is an optical non-destructive testing technology that uses laser refraction and reflection inside the object to reflect its internal information. Biospeckle imaging equipment and image processing algorithms are constantly improved, and the application fields are gradually expanding. Due to the existence of interference factors, the precision of modelling is still the focus of researchers at present. The speckle image processing algorithm is reviewed in detail, and the application of biospeckle technology in fruit quality detection is investigated. The main imaging equipments are summarized and suggestions for improvement are proposed to provide inspiration for future research.

Key words laser optics; biospeckle; fruit quality detection; laser speckle; imaging processing algorithm

OCIS codes 140.7300; 110.6150; 110.2960; 140.3460

1 引 言

生物散斑法是一种基于激光照射到生物样品产生相干光的光学无损检测技术，可以在观察面上看到由散射射线相互干扰而形成的、由暗斑和光点组成的随机的颗粒状图案。散斑图像取决于样本的形状、激光器的波长和捕捉装置的透镜孔径，包含两个内容：静态和动态。静态图像来自生物样品的静态部分，动态图像产生于组织中粒子或分子的移动。激光能够与移动的粒子相互作用，因此可以对由光的多普勒变换引起的散斑图像的动态变化进行统计分析[1]。散斑活动受生物体生理和化学反应过程中细胞质流、细胞器运动、生长和分裂的影响。在植物体中，散斑活动还与叶绿素含量[2]、淀粉含量[3]、真

收稿日期：2018-09-07；**修回日期**：2018-10-08；**录用日期**：2018-11-27

基金项目：上海市农委科研项目(18H100000210)、上海市科委项目(15391912600)、上海市果业产业技术体系

* **E-mail**：acaizh@sjtu.edu.cn；** **E-mail**：wp-xu@sjtu.edu.cn

菌感染[4]、温度[5]等因素有关。

生物散斑可以提供关于细胞内各种生命过程的信息，在植物上的应用范围很广[6-11]。胡孟晗等[12]在之前的一篇文章中详细介绍了静态散斑与动态散斑在农产品中的各项应用，但对建模方法阐述较少。本文主要介绍生物散斑的图像处理算法，整理其在水果上的应用和相关散斑成像设备。

2 生物散斑成像设备类型

相比于其他无损检测成像设备，生物散斑成像装置较为简单，一般分为反射型和透射型。用于测量生物散斑的基本设备由能够发射均匀照亮物体表面相干光的激光器、CCD 相机、计算机组成。CCD 相机获取散斑图像后传到计算机，经过软件分析后便可获取各种生物信息。

图 1 总结了几种常用的成像设备，其中图 1(a)、(b)、(c)是反射型成像设备，图 1(d)是透射型成像设备。各型设备的基本工作原理简述如下：1) 如图 1(a)所示，利用光束扩大镜将激光束直径放大，从而相机获得样品上更大范围的光斑；2) 如图 1(b)所示，利用反光镜反射激光至样品，并不直接使激光打在样品上；3) 如图 1(c)所示，通过衰减器使样品上的光斑亮度降低，再用扩散器放大反射光的直径，丰富散斑图像细节。测量生物散斑应考虑激光波长、样品与相机的距离和角度、偏振和光强，以及相机光圈。Zdunek 等[13]以苹果为材料，认为目标的光圈大小使得散斑直径由公式 $d=1.22(\lambda z/D)$ 决定，其中，λ 为激光波长，z 为观测距离，D 为光照区直径。物体表面静态散斑的大小取决于光入射角度，而由组织内部产生的较小的动态散斑与角度无关。

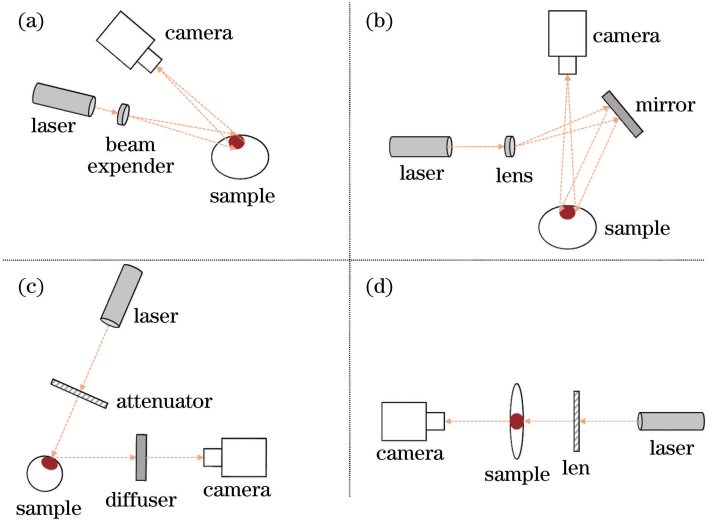

图 1 生物散斑测量实验设备。(a)基于光束扩大镜的反射型成像；(b)基于反光镜的反射型成像；(c)基于衰减器和扩散器的反射型成像；(d)透射型成像

Fig. 1 Experimental setup for biospeckle measurements. (a) Reflection imaging based on beam expander; (b) reflection imaging based on reflector glass; (c) reflection imaging based on attenuator and diffuser; (d) transmission imaging

2.1 反射型生物散斑成像设备

反射型成像设备激光器与相机在同一侧，主要接收由物体反射的光线。激光进入物体内部，经过折射和反射最终呈现在物体表面，相机则记录反映在物体表面的光斑。反射光与入射光的夹角较小，一般用于难以透光的样本，如苹果[2]、柑橘[14]、杧果[15]等。研究表明[16-18]，在基础设备上增加扩束镜、镜子、衰减器、柔光镜等装置可以获取更好的图像效果。

2.2 透射型生物散斑成像设备

透射型成像设备较多用于能够透光的样本。激光穿透物体，相机在样本背面接收透射光，以便获取更加完整的信息，减少外部因素的干扰。样品厚度越小，透射成像效果越好[19]。但是，在实际使用中透射型水果样品处理极不方便，并且违背了生物散斑检测无损、快速的特点，因此本文不过多阐述透射型成像的应用。反射型设备与透射型设备的优缺点及其应用范围归纳如表 1 所示。

3 生物散斑在不同水果中的应用

根据获取图像的方式，散斑图像分为动态散斑和静态散斑两种，通常以采集图像时长是否大于等于 1 s 来划分。静态散斑的获取通常只需要拍摄几幅图像，采集时长小于 1 s，通过常规的图像处理方

法分析散斑图像。动态散斑通常获取一段大于等于1 s的视频，利用时间或空间上散斑的变化对图像序列进行分析[20]。生物散斑可以应用于区域识别、果肉质地区分、微生物感染、生理指标检测等方面。

表1 反射型设备与透射型设备的优缺点及其应用

Table 1 Advantages and disadvantages of reflection equipment and transmission equipment and their applications

Type	Advantage	Disadvantage	Application
Reflection	Simple sample processing; wide range of applications	Physiological differences between samples; larger sampling error	Quality identification, damage, fungi infection, etc.
Transmission	Same sample processing; smaller error between samples; more realistic information	Sample preparation is more complicated; experimental results may differ from actual use	Sample of good transmission

3.1 区域识别

Pajuelo等[21]用波长633 nm的激光照射苹果的受撞击部位，发现苹果受到撞击的部位散斑活动少于未受撞击的部位，且受到撞击的部位散斑活动在1 d后明显降低。Kumari等[22]用基于强度的算法区分9 d货架期期间苹果的受损和新鲜区域，发现惯性矩法计算得到的受损区域和新鲜区域之间的生物散斑活动总体差异最大。Samuel等[23-26]也对苹果的受损区域进行了分析。

刘海彬等[27]分别采集皇冠梨缺陷部位、花萼、果梗、无缺陷部位的散斑图像，利用Fujii法和加权广义差分法对512幅散斑图像进行分析，用灰度共生矩阵特征提取16组特征量，结果表明，利用生物散斑法可以对梨缺陷部位、果梗、花萼进行识别。Vega等[25]也对梨的受损区域进行了分析。

Retheesh等[28]应用波长为632.8 nm的激光识别绿色柑橘表皮的疤痕区域，通过与常规方法对比，验证了该方法的有效性。Samuel等[23]对柑橘的损伤变化进行了分析。

在杧果[23]、草莓[29]、香蕉[30-31]等水果上也进行了机械损伤及冻伤相关的识别工作。

3.2 果肉质地区分

Arefi等[32]分别记录波长680 nm和780 nm照射下25 s的生物散斑活动，对苹果新鲜、半粉状和粉状这三个性状进行了分类，在此基础上又将视频细分为1，2.5，5，15，25 s来对比预测精确度[33]。但作者也提到，拍摄时间过长是阻碍其实际应用的弊端。

3.3 微生物感染

Adamiak等[4]对不同条件贮藏期间和后续保质期间的苹果牛眼果腐病的发展和苹果品质进行了监测，以及采前品质测定，认为可以用生物散斑法预测苹果的收获期[34]，用生物散斑、高光谱成像和叶绿素荧光三种方法分别对储存的苹果真菌感染进行早期检测，发现生物散斑活动的空间可视化揭示了疾病的发展，且比超光谱成像更加精细，较叶绿体荧光法能够更早地检测到感染[35]。作为易腐坏水果，草莓[20]等相关研究也受到了关注。

3.4 生理指标检测

Romano等[36]连续监测干燥过程中苹果的硬度、含水量和可溶性固形物含量的变化，发现随着含水量下降，可溶性固形物含量增加，光子散射减少，散射图像显示出较少的光子迁移。虽然该方法对可溶性固形物含量的预测准确度略低，但足以预测苹果含水量和可溶性固形物含量的变化。然而不建议用该方法预测干燥过程中苹果的硬度变化。

Zdunek等[3]研究了苹果的硬度、可溶性固形物含量、可滴定酸和淀粉含量、叶绿素含量[2]、温度[5]、细胞松弛素B、微丝解聚素B、秋水仙碱、环己酰亚胺、二甲基亚砜和离子通道抑制剂[37]，以及静水压力[38]对苹果散斑活动的影响。提出对生物散斑空间活动的Fujii指数加倍平滑可以得到高对比度的生物散斑活动图像，且散斑图像分辨率没有任何损失[39]。

苹果[40-48]、梨[40-45,49-50]、番石榴[41]、柑橘[23,51]、番茄[40,42-44]、草莓[52]、杧果[15,23]、香蕉[53]、李子[54-55]、西瓜[56]、木瓜[57]、甘蔗[58]、柠檬[59]、猕猴桃[60]、百香果[61]、桃[62]等进行了相关研究。

3.5 小结

表2详细总结了生物散斑在水果中的各类应用，并且列出了每个实验中测量散斑活动的方法以及分析散斑活动变化的算法，表中使用所述相关系数$C^{k\tau}$对散斑活动进行评估，其k是帧号，τ是滞后时间。激光波长和激光器的选择与水果的种类、性状有关，样品对激光的吸收与反射会直接影响散斑图像的成像效果。要使散斑活动尽可能真实地反映

表 2 生物散斑活动的应用及其算法总结

Table 2 Summery of applications of biospeckle activities and relative algorithms

Reference	Application	Wavelength /nm	Measures and analysis of biospeckle activity	Sample
[21]	Assessment of bruising	633	Time history speckle pattern, inertia moment, weighted generalized difference, laser speckle contrast analysis method, Fujii	Apple
[22]	Differentiation of bruised and fresh regions	632.8	Inertia moment, absolute value difference, generalized difference, parameterized Fujii, biospeckle activity value, granulometric size distribution, grey-level co-occurrence matrix, parameterized generalized difference, alternative generalized difference, parameterized global average Fujii	Apple
[23]	Quality evaluation and damage identification	632.8	Time history speckle pattern, inertia moment, cross-correlation coefficient C, generalized difference	Apple
[24]	Evaluation of damages	633	Time history of speckle pattern, cross correlation	Apple
[25]	Detection of bruises	633	Time history of speckle pattern, autocorrelation function, weightedgeneralized difference	Apple
[26]	Identificationof early bruising	632.8	Fujii, generalized difference, laser speckle contrast analysis	Apple
[32]	Identification of mealy apples	680,780	Time history speckle pattern, autocorrelation function, inertia moment, absolute value of differences	Apple
[33]	Identification of mealy apples	680,780	Time history of speckle pattern, artificial neural networks	Apple
[4]	Development of bull's eye rot and quality changes	632.8	Correlation coefficient $C^{k\tau}$	Apple
[34]	Pre-harvest monitoring	635	Correlation coefficient $C^{k\tau}$	Apple
[35]	Early detection of fungal infection	473, 532, 830	Fujii, correlation coefficient $C^{k\tau}$, inertia moment, method based on frequency analysis	Apple
[36]	Monitor soluble solid content, moisture content, hardness	635	Gray value, RGB(red, green, blue) pixel value	Apple
[3]	Quality evaluation	632	Correlation coefficient $C^{k\tau}$	Apple
[2]	Chlorophyll content	670	Correlation coefficient $C^{k\tau}$	Apple
[5]	Temperature effect on biospeckle activity	632.8	Correlation coefficient $C^{k\tau}$, speckle contrast, inertia moment	Apple
[37]	Effect of cytochalasin B, lantrunculin B, colchicine, cycloheximid, dimethyl Sulfoxide and ion channel inhibitors	635	Correlation coefficient, laser speckle contrast analysis	Apple

续表

Reference	Application	Wavelength /nm	Measures and analysis of biospeckle activity	Sample
[38]	Four optical methods to measure hydrostatic pressures	635, 690, 830, 1060	Correlation coefficient $C^{k\tau}$	Apple
[39]	Comparison of new methods and traditional methods to identify fungal infections	532	Fujii, motion history images, exponentially smoothed Fujii	Apple
[40]	Measurement of biospeckle activities during storage in 7 days	632.8	Spatial-temporal speckle correlation, inertia moment	Apple
[41]	Biospeckle activity measurement during shelf-life storage	632.8	Correlation coefficient $C^{k\tau}$	Apple
[42]	Biospeckle activity measurement during storage	632.8	Correlation coefficient $C^{k\tau}$	Apple
[43]	Biospeckle activity measurement	632.8	Time history of speckle pattern, inertia moment, absolute value of differences	Apple
[44]	Biospeckle activity measurement during shelf-life storage	632.8	Time history of speckle pattern, inertia moment, absolute value of differences	Apple
[45]	Biospeckle activity measurement during shelf-life storage	632.8	Generalized difference, Fujii, alternative Fujii	Apple
[46]	Effect of edible filmson apple quality	632	Inertia moment	Apple
[47]	Different feature extraction of evaluation of firmness	680, 780	Time history of speckle pattern, inertia moment, absolute value of differences, wavelet, artificial neural networks	Apple
[48]	Climacteric peak	632.8	Correlation coefficient C	Apple
[40]	Measurement of daily biospeckle activities during storage	632.8	Spatial-temporal speckle correlation, inertia moment	Pear
[41]	Biospeckle activity measurement during shelf-life storage	632.8	Correlation coefficient $C^{k\tau}$	Pear

续表

Reference	Application	Wavelength /nm	Measures and analysis of biospeckle activity	Sample
[42]	Biospeckle activity measurement during storage	632.8	Correlation coefficient $C^{k\tau}$	Pear
[43]	Biospeckle activity measurement	632.8	Time history of speckle pattern, inertia moment, absolute value of differences	Pear
[44]	Biospeckle activity measurement during shelf-life storage	632.8	Time history of speckle pattern, inertia moment, absolute value of differences	Pear
[45]	Biospeckle activity measurement during shelf-life storage	632.8	Generalized difference, Fujii, alternative Fujii	Pear
[27]	Detection of stem/calyx and defect	635	Fujii, weighted generalized difference	Pear
[49]	Ripening detection	632.8	Auto-covariance function	Pear
[50]	Maturation detection	632.8	Auto-covariance function	Pear
[25]	Detection of bruises	633	Time history of speckle pattern, autocorrelation function, weighted generalized difference	Pear
[28]	Identification of scar region	632.8	Fujii, temporal difference, laser speckle contrast analysis, generalized difference, motion history image	Orange
[51]	Measurement of peel thickness	633	Size of laser beam	Orange
[23]	Quality evaluation and damage identification	632.8	Time history speckle pattern, inertia moment, cross-correlation coefficient C, generalized difference	Orange
[40]	Measurement of biospeckle activities during storage	632.8	Spatial-temporal speckle correlation, inertia moment	Tomato
[42]	Biospeckle activity measurement during storage	632.8	Correlation coefficient $C^{k\tau}$	Tomato
[43]	Biospeckle activity measurement	632.8	Time history of speckle pattern, inertia moment, absolute value of differences	Tomato
[44]	Biospeckle activity measurement during shelf-life storage	632.8	Time history of speckle pattern, inertia moment, absolute value of differences	Tomato
[20]	Detection of bruised areas and fungal development	650	Generalized difference, Fujii, speckle noise	Strawberry
[52]	Maturation detection	632.8	Time history of speckle pattern, correlation coefficient function	Strawberry
[29]	Maturation detection	Unknown	Mobility index	Strawberry

续表

Reference	Application	Wavelength /nm	Measures and analysis of biospeckle activity	Sample
[15]	Maturation detection	632	Time history of speckle pattern, inertia moment, two-dimensional cross correlation function	Mango
[23]	Quality evaluation anddamage identification	632.8	Time history speckle pattern, inertiamoment, cross-correlation coefficient C, generalized difference	Mango
[53]	Chlorophyll index, elasticity, soluble solid contents	532, 660, 830	Artificial neural network, support vector machine	Banana
[30]	Detection of chilling injury symptoms	785	RGB values	Banana
[31]	Chilling injury	660, 785	RGB values	Banana
[55]	Changes in backscattering imaging before and after harvest	532, 785	Gaussian-Lorentzian cross product function	Plum
[54]	Quality	785	Lorentzian distribution function	Plum
[56]	Identification of seeded and seedless watermelon	658	Linear discriminant analysis, quadratic discriminant analysis, k-nearest neighbour	Watermelon
[57]	Monitoring of quality changes during drying	532, 650, 780	Extract illuminated area and light intensity profile	Papaya
[58]	Water content and sugar content	632	Time history of speckle pattern, inertia moment	Sugar cane
[59]	Assessment of biospeckle activity	Unknown	Time history of speckle pattern, inertia moment, correlation coefficient $C^{k\tau}$	Lemon
[60]	Laser light propagation	785	Monte Carlo simulation	Kiwi fruit
[61]	Adsorption behavior	632	Variable moment of inertia	Passion fruit
[41]	Measurement of biospeckle during shelf-life storage	632.8	Correlation coefficient $C^{k\tau}$	Guava
[62]	Firmness	Unknown	Partial least squares regression, least squaressupport vector machines	Peach

在相机中，减少外界干扰，就需要选择合适的波长进行实验。此外，相机的对焦模式也会影响散斑活动的拍摄效果，自动对焦偶尔会在拍摄时失焦，给后期图像处理带来不便。以柑橘等果皮较厚、易产生浮皮的水果作为样品时，必须考虑果皮厚度对光线在果实中传播造成的误差。在市场中购买水果会遇到打蜡的情况，要注意果蜡对光线的影响。对于容易腐烂、保质期较短的水果应该着眼于病菌侵染、损伤的早期检测。上述因素对激光生物散斑技术在水果检测领域应用结果的影响还需进一步的优化。

4 生物散斑图像处理算法

4.1 静态散斑图像处理算法

激光束在两个没有可见缺陷的位置上获取后向散射图像。由于激光在水果组织中的迁移，靠近入射激光点表面的周围区域均被照亮。每个图像选择照明面积，使用 Adobe CS3 PS 图象处理软件处理并进行软件计算分析。对于每一张图片，计算的指

标包括这些激光参数、散射面积(A635)的像素数、冷光(L635)对应的照明区域灰度值[范围由 0(黑)至 255(白)]。计算 RGB 像素值,公式为[11]

$$L_{635}=0.3\times R+0.6\times G+0.1\times B, \tag{1}$$

式中:R、G、B 为色素灰度的三个分量。

使用统计软件进行校准和验证。计算散射参数和参考值之间相关性的确定系数;建立最佳拟合激光参数的预测模型,并用单交叉验证法进行验证。计算交叉验证的标准误差 S_{ECV},以评估每个模型的预测能力[36]。

$$S_{\mathrm{ECV}}=\sqrt{\frac{\sum_{i=1}^{n_1}(\bar{y}_{\mathrm{p}i}-y_i-B_{\mathrm{ias}})^2}{n_1-1}}, \tag{2}$$

$$B_{\mathrm{ias}}=\frac{\sum_{i=1}^{n_1}(\bar{y}_{\mathrm{p}i}-y_i)}{n_1}, \tag{3}$$

式中:$\bar{y}_{\mathrm{p}i}$ 代表激光预期值的平均值;$y_{\mathrm{p}i}$ 代表激光的预期值;y_i 代表测量值;n_1 为样本总数;i 为像素点编号;B_{ias} 代表测量值和预测值的差异。

4.2 动态散斑图像处理算法

4.2.1 激光散斑空间对比分析(LASCA)法

空间对比分析法[1]通过单一散斑图取窗口测对比值,能快速处理每一张图像并分别得到一张结果图,可实现实时监测[63]。在一张散斑图中取一个小窗口(窗口大小多为 3 pixel×3 pixel、5 pixel×5 pixel 或 7 pixel×7 pixel)。令 $f(x,y)$ 为 (x,y) 点处的灰度值。若是一张图为 8 bit,则 $f(x,y)$ 对应的取值范围是 0~255。取 (x,y) 点处的一个方形邻域窗口 $(x+a,y+b)$,其对应灰度值是 $f(x+a,y+b)$。其中:$-m<a<m$,$-m<b<m$,a、b 为窗口内横纵坐标轴上窗口内的任取值,m 为 (x,y) 点至窗口边缘所含像素数,若选定窗口大小为 3 pixel×3 pixel,则 m 值为 1。

窗口边长为

$$l=2m+1。 \tag{4}$$

窗口面积为

$$L=l^2=(2m+1)^2。 \tag{5}$$

该窗口内全部像素点灰度值的平均值为

$$\bar{I}(x,y)=\frac{\sum_{a=-m}^{m}\sum_{b=-m}^{m}f(x+a,y+b)}{L}。 \tag{6}$$

全部像素点灰度值的标准差为

$$\sigma_{\mathrm{s}}(x,y)=\sqrt{\frac{\sum_{a=-m}^{m}\sum_{b=-m}^{m}[f(x+a,y+b)-\bar{I}]^2}{L}}。 \tag{7}$$

令 K 为该窗口灰度的对比值,即 K 是窗口中所有像素点灰度值标准差与所有像素点灰度平均值的比值,即:

$$K=\frac{\sigma_{\mathrm{s}}(x,y)}{\bar{I}(x,y)}=\frac{\sqrt{\frac{\sum_{a=-m}^{m}\sum_{b=-m}^{m}[f(x+a,y+b)-\bar{I}]^2}{L}}}{\frac{\sum_{a=-m}^{m}\sum_{b=-m}^{m}f(x+a,y+b)}{L}}。 \tag{8}$$

令窗口按照由左至右、由上至下的顺序移动,得到所有窗口的灰度对比值 K,再依次将这些值作为所构建图像中对应像素点的像素值,构建所得图像即为处理图。

LASCA 法的优点是处理的数据量较少,只需一幅图像就可获得处理图;缺点是所得处理图清晰度较低,另外,还须小心选择相机曝光时间,否则难以获得满意的成像效果[64]。

4.2.2 时间序列散斑(THSP)图像

目前常用的图像处理方法大都是针对时间序列散斑图像的。THSP 展现了散斑图中一固定列(或行)上像素点的变化。在初始图像中选定一固定行(多选取中心行或活动最剧烈处)作为第一行,之后按顺序提取每一副散斑图像中的该列(或行),依次排列成时间序列散斑图[18]。

4.2.3 广义差分(GD)法

时间序列散斑图表现图像中某一列(或行)的变化,而 GD 法则对所有的像素点进行统计处理,得到其总体变化的统计结果。定义式为[22]

$$D_{\mathrm{G}}=\sum_{i_1=0}^{n_2-1}\sum_{i_2=i_1+1}^{n_2-1}|x_{i_1}-x_{i_2}|, \tag{9}$$

式中 i_1、i_2 为选定列(行)中像素点的编号(像素点按次序依次编号);x_{i_1}、x_{i_2} 为 i_1、i_2 点的坐标,取值范围为 0~(n_2-1),n_2 为该散斑图总帧数;广义差分 D_{G} 为强度差的加值。式中取绝对值的部分代表图中某一固定点不同时刻强度变化的差值。

某一点的灰度值变化越大,说明该点不同时刻的强度的差值越大。叠加差值,便能得到点与点之间的强度变化的差异。

4.2.4 Fujii 法

Fujii 法又称为 Average Difference,与 GD 法类似,计算时间相邻的两幅图之间每一点的灰度值强度差的加权和,通过处理结果可以看出不同点的强

度变化的差别[65]。

其定义式为

$$D_{(n_3)}=\sum_{t=1}^{n_3-1}\frac{|I_{t(i_3)}-I_{t+1(i_3)}|}{|I_{t(i_3)}+I_{t+1(i_3)}|},\tag{10}$$

式中：I 为某一时刻(某一帧)的灰度值，即 $I_{t(i_3)}$ 为 t 时刻 i_3 点的灰度值；n_3 为该散斑图图像总帧数，t 为不同的时刻(帧数)，其取值范围为 $1\sim(n_3-1)$。

4.2.5 激光散斑时间对比分析(LSTCA)法

LSTCA 法[1]的定义式为

$$C_{x,y}=\frac{\sqrt{\frac{1}{n_4-1}\sum_{t=t_0}^{T}I_{x,y}^{t}-\bar{I}_{x,y}}}{\bar{I}_{x,y}},\tag{11}$$

式中：x、y 为某一点的横纵坐标；t 为不同的时刻(帧数)，取值范围为 $t_0\sim T$，t_0 为起点时刻，T 为总时间，即终点时刻；n_4 为图像总数；$I_{x,y}^{t}$ 为 (x,y) 点 t 时刻(第 t 帧)的像素值；$\bar{I}$ 为全体图像中该固定点的平均灰度值。

该法与空间对比分析法相似，但通过分析散斑图中每一像素点在一段时间内的变化来得到对比图像。实验证明，其分辨率可达到空间对比方法中图像分辨率的 5 倍[66-68]。

4.2.6 传统惯性矩(IM)法

惯性矩分析[15]是一种以时间序列散斑图为基础的处理方法。

对于一幅时间序列散斑图，其共生矩阵为

$$C_{\mathrm{OM}}=[N_{I_1,I_2}],\tag{12}$$

式中：I_1、I_2 为元素的某一灰度值；N 表示在元素值 I_1 后面接着出现元素值 I_2 的次数。

共生矩阵原理：对一幅时间序列散斑图来说，设元素 I_1 后继续出现元素 I_2 次数共为 N 次，将 N 值赋给该共生矩阵中第 I_1 行、第 I_2 列的元素。如图 2 所示，在元素 1 之后出现元素 2 的次数为 2，故第 1 行第 2 列的值为 2；同理，第一行第一列的值为 1。

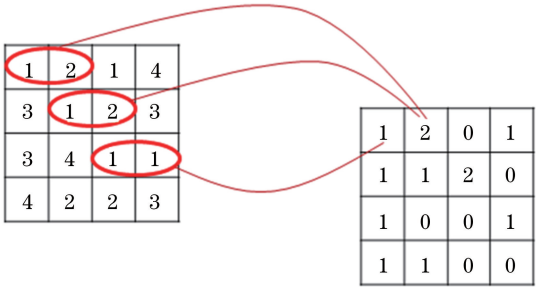

图 2 共生矩阵的构建过程

Fig. 2 Process of symbiotic matrix construction

张明捷等[69]利用非主对角线上非零元素个数及其偏离主对角线的距离表示散斑活性，

$$M_{I_1,I_2}=\frac{N_{I_1I_2}}{\sum_{I_2}N_{I_1I_2}},\tag{13}$$

式中：M_{I_1,I_2} 为 $N_{I_1I_2}$ 发生概率。

$$M_{I_1}=\sum_{I_1I_2}M_{I_1I_2}(I_1-I_2)^2,\tag{14}$$

式中：M_{I_1} 为非零元素 I_1 偏离主对角线的程度，即散斑活性(I_{M} 值)。对于不同强度变化的时间序列散斑求其 I_{M} 值，即可定量分析其生物体活性程度。

4.2.7 改进惯性矩(IM)法

传统的惯性矩分析算法有其优势，但也存在着稳定性较低、易于出现异常值等缺点，行(列)的选取方式会严重影响实验结果的准确性和稳定性，所取行(列)需要具有代表性。因此，蔡健荣等[70]提出了两个方向的改进，即惯性矩算法的改进和代表行选取的改进。

在实验过程中可能由于移动样本、样本表面形变且不规则等原因，导致光强最高峰位置产生一定的偏移。如果取某一固定行(列)求样本的 I_{M} 值，其结果可能存在着一定误差。因此，在得到最高峰位置后，选取其与其周围相邻两行，将三行 I_{M} 均值作为样本 I_{M}。

蔡健荣等[70]认为由于噪音等因素的存在，可能会出现个别异常的像素灰度值，导致 I_{M} 值异常，提出以下两种改进方式。

1) 修正矩阵(MCOM)算法的改进。传统算法是求共生矩阵中每个像素灰度值在所在行或列中的权重。改进的公式为

$$M'_{I_1I_2}=\frac{N_{I_1I_2}}{\sum_{I_1I_2}N_{I_1I_2}},\tag{15}$$

式中：$\sum_{I_1I_2}N_{I_1I_2}$ 代表矩阵图中灰度值总和；$M'_{I_1I_2}$ 代表每一对应像素点灰度值与矩阵总和的对比值，即使出现异常点，其权重相比传统算法要小，减小了干扰力度。

2) 对非零元素偏离对角线距离的改进。为了更好地体现出矩阵中不同非零元素偏离主对角线距离间的差异，将非零元素偏离对角线地距离的平方作为改进后的 I_{M} 值，公式为

$$M_I=\sum_{I_1I_2}\frac{M'_{I_1I_2}(I_1-I_2)^2}{2}。\tag{16}$$

4.2.8 时间差分(TD)法

TD 法[71]是另一种前景光明的图像处理方式。

Fujii 法只能描述整个观测期的整体斑点活动，缺少其活动的演化过程。时间差分法的主要优势是可以按照时间顺序记录散斑活动结果。

TD 法通过计算由时间分隔的连续图像的绝对差值得到散斑图。计算公式为

$$T_{\mathrm{D}}(x,y)=\sum_{t=1}^{n_5-1}\left|I_t(x,y)-I_{t+1}(x,y)\right|,\tag{17}$$

式中：t 为不同的时刻(帧数)，范围为 1～(n_5－1)，n_5 为图像总帧数；$I_{t(x,y)}$ 代表图中 t 时刻(x，y)位置的像素值。

4.2.9 绝对差分(AVD)法

AVD 法主要作为常规 IM 法的替代方案。它基于以下原则：差异的总和是搜索的主要信息，并且在 IM 法中执行的平方操作能够以失真的方式放大时间历史的变化[72]。定义式为

$$A_{\mathrm{VD}}=\sum_{I_1I_2}\left(C_{\mathrm{OM}}[I_1,I_2]\times\left|I_1-I_2\right|\right),\tag{18}$$

式中：I_1、I_2 为元素的某一灰度值；$C_{\mathrm{OM}}[I_1,I_2]$为对应的共生矩阵。

4.2.10 JC 法

该算法基于对散斑图的直接处理，不需要其他类型的后处理(如 THSP 和共生矩阵)，是一种可行的实时方法[73]。

在时间 T 内取一组分开的图像，其时间间隔为 $1/f$，其中 f 是相机采集帧的速率。设一像素点的坐标为(x，y)，正面左下角坐标为(1，1)，右上角坐标为(w，h)。w、h 各为总宽度、总高度中包含的像素数，记录时刻 t 在(x，y)处的像素值为 $I_{xy,t}$，t 的范围为 1～T。

强度的变化可划分为两部分：1) 缓慢变化的部分 $P_{xy,t}$，代表背景温度波动和其他缓慢变化产生的低频噪声；2) 迅速变化的部分 $S_{xy,t}$，包含目标信号。因此，时刻 t 的像素值可表示为

$$I_{xy,t}=P_{xy,t}+S_{xy,t}。\tag{19}$$

在 X(设 $X<T$)幅图像上逐个对像素进行强度求和，X 为任取的适当较小值，从时刻 t 开始，定义

$$J_{\mathrm{C}_{xy}}(X)=\sum_{t=1}^{T-X}\left|S_{xy,t+1}+S_{xy,t}\right|=\sum_{t=1}^{T-X}\left|\frac{I_{xy,t}I_{xy,t+1}-\left(\sum_{t=1}^{T-X}\frac{I_{xy,t+1}}{X}\right)^2}{\sum_{t=1}^{T-X}\frac{I_{xy,t+1}}{X}}\right|。\tag{20}$$

它将不同像素的强度值相关联，得到定性的图像处理结果，并表现出每个像素的高强度和低强度变化。对于定量情况，可以假设散斑图案是随机但均匀分布在整个图像上的(例如客观散斑图案)，计算图像子区域上 $J_{\mathrm{C}_{xy}}(X)$的平均值。获得$\Delta J_{\mathrm{C}_{xy}}(X)$为

$$\Delta J_{\mathrm{C}_{xy}}(X)=\left|\frac{1}{WL}\sum_{x=1}^{W}\sum_{y=1}^{L}\sum_{t=1}^{X-1}\frac{I_{xy,t}I_{xy,t+1}-\left(\sum_{j=0}^{X-1}\frac{I_{xy,t+1}}{X}\right)^2}{\sum_{j=0}^{X-1}\frac{I_{xy,t+1}}{X}}\right|,\tag{21}$$

式中：W、L 为选定子区域的总宽度和总长度，范围分别为 0～w、0～h。

4.3 总　　结

以上算法是国内外常用的生物散斑处理算法。表 2 将实际案例的常用算法整理在了表格的第三列，表 3 比较了以上 10 种算法，其中，将传统惯性矩法和改进惯性矩法统一作为 IM 算法与其他算法进行比较。

LASCA 法的优点是处理快速实时、数据量小，通过一幅图就可获得处理图，缺点是所得处理图清晰度较低，而且需需要小心选择相机曝光时间，否则难以获得满意的成像效果。THSP 主要作为 IM 法的预处理存在，行的选取应具有代表性，否则误差较大。GD 法也可作为图像预处理方法，通过对所有像素点进行统计，获取总体变化。Fujii 法与 GD 法类似，处理过程简单。LSTCA 与 LASCA 法类似，但其分析一段时间内的变化，相应处理得到的图像分辨率远远高出 LASCA 法，但无法实时处理。IM 法以 THSP 为基础，需要设置共生矩阵，流程相对复杂，无法实时处理，但精确度高，是较为常用的一种处理算法，有许多研究者对其进行改进。TD 法可以展示出整个观测时期散斑活动的演变过程。AVD 法作为 IM 法的补充方案，放大了图像的变化差值。JC 法是新出现的一种处理方法，可直接处理，抗干扰能力强。

4.4 展　　望

散斑技术是一种成本低、快速、实时的，可定性或定量的无损检测方式。它的出现时间还比较短，在水果品质检测方面具有广泛的应用前景。上文列出了 10 种散斑图像处理算法，而现在依然有许多研究者致力于改进这些算法或开发新算法。改进算法包括以下方面：1) 缩短图像采集时间，如同时从多个角度进行图像采集，对其进行融合处理；2) 提高抗干扰能力，样本的位置、形状，以及光线等均会对结果产生影响，新算法应减少这些因素对结果的干扰；3) 结合实际运用，根据需要的指标，针对性地进行处理，考虑不同果实的复杂结构；4) 提高处理精确度。

表 3 动态散斑处理算法对比

Table 3 Comparison of dynamic speckle processing algorithms

Feature	LASCA	THSP	GD	Fujii	LSTCA	IM	TD	AVD	JC
Real-time processing	Yes	No	No	No	No	No	No	No	Yes
Object	All pixels	A line	All pixels	All pixels	All pixels	A line	All pixels	A line	All pixels
Qualitative(qual)/ quantitative(quan)	Qual	Qual	Qual	Qual	Qual	Quan	Qual	Quan	Quan

5 结束语

植物果实是植物的重要组成部分，果实品质由外观品质、风味品质、营养品质、加工品质和贮藏品质等多方面因素综合组成。对植物果实的可视化研究，可以预测果实成熟时间，有利于采摘等管理安排，还可以为果实的分级提供理论基础，通过走标准化生产道路，进行果品等级调整，助力产业升级和可持续发展。

综述了生物散斑的成像设备、在水果上的应用以及各种图像处理数学方法。散斑活动受到果实内部各种生理活动及外界环境的影响，利用图像处理软件和数学方法解析散斑活动后建立模型能够有效地反映果实的状态。将这种无损检测的方法应用到生产实际中能够极大程度地提高检测效率，且不会破坏果实的完整性。如果将成像模块、分析模块集成到一起，可以进一步拓展该技术的应用场景。

参 考 文 献

[1] Draijer M, Hondebrink E, van Leeuwen T, *et al*. Review of laser speckle contrast techniques for visualizing tissue perfusion[J]. Lasers in Medical Science, 2009, 24(4): 639-651.

[2] Zdunek A, Herppich W B. Relation of biospeckle activity with chlorophyll content in apples[J]. Postharvest Biology and Technology, 2012, 64(1): 58-63.

[3] Zdunek A, Cybulska J. Relation of biospeckle activity with quality attributes of apples[J]. Sensors, 2011, 11(6): 6317-6327.

[4] Adamiak A, Zdunek A, Kurenda A, *et al*. Application of the biospeckle method for monitoring bull′s eye rot development and quality changes of apples subjected to various storage methods: preliminary studies[J]. Sensors, 2012, 12(3): 3215-3227.

[5] Kurenda A, Adamiak A, Zdunek A. Temperature effect on apple biospeckle activity evaluated with different indices[J]. Postharvest Biology and Technology, 2012, 67: 118-123.

[6] Braga R A, Dupuy L, Pasqual M, *et al*. Live biospeckle laser imaging of root tissues[J]. European Biophysics Journal, 2009, 38(5): 679-686.

[7] Salambue R, Adnan A, Shiddiq M. Investigation of the ripeness of oil palm fresh fruit bunches usingbio-speckle imaging[J]. Journal of Physics: Conference Series, 2018, 978: 012071.

[8] Dhanotia J, Bopche L, Bhatia V, *et al*. Quality assessment of medicinal leaves through biospeckle technique[M]// Dhanotia J, Bopche L, Bhatia V, *et al*. Springer Proceedings in Physics. Singapore: Springer Singapore, 2017: 389-394.

[9] Vivas P G, Resende L S, BragaJr R A, *et al*. Biospeckle activity in coffee seeds is associated non-destructively with seedling quality[J]. Annals of Applied Biology, 2017, 170(2): 141-149.

[10] Madjarova V, Toyooka S, Nagasawa H, *et al*. Blooming processes in flowers studied by dynamic electronic speckle pattern interferometry (DESPI)[J]. Optical Review, 2003, 10(5): 370-374.

[11] Romano G, Argyropoulos D, Nagle M, *et al*. Combination of digital images and laser light to predict moisture content and color of bell pepper simultaneously during drying[J]. Journal of Food Engineering, 2012, 109(3): 438-448.

[12] Hu M H, Dong Q L, Liu B L, *et al*. Application of biospeckle on analysis of agricultural products quality[J]. Transactions of the Chinese Society of Agricultural Engineering, 2013, 29(24): 284-292.
胡孟晗, 董庆利, 刘宝林, 等. 生物散斑技术在农产品品质分析中的应用[J]. 农业工程学报, 2013, 29(24): 284-292.

[13] Zdunek A, Adamiak A, Pieczywek P M, *et al*. The biospeckle method for the investigation of agricultural crops: a review[J]. Optics and Lasers in Engineering, 2014, 52: 276-285.

[14] Rabelo G F, Braga Jr R A, Fabbro I M D. Laser speckle techniques in quality evaluation of orange fruits[J]. Revista Brasileira de Engenharia Agrícola e Ambiental, 2005, 9(4): 570-575.

[15] Retheesh R, Samuel B, Radhakrishnan P, *et al*. Use of laser biospeckle for the evaluation of fruit ripening [J]. Journal of Pure Applied and Industrial Physics, 2016, 6(5): 65-70.

[16] Skic A, Szymańska-Chargot M, Kruk B, *et al*. Determination of the optimum harvest window for apples using the non-destructive biospeckle method [J]. Sensors, 2016, 16(5): 661.

[17] Alves J A, Braga Jr R A, Vilas Boas E V. Identification of respiration rate and water activity change in fresh-cut carrots using biospeckle laser and frequency approach [J]. Postharvest Biology and Technology, 2013, 86: 381-386.

[18] Romero G G, Martinez C C, Alanís E E, *et al*. Biospeckle activity applied to the assessment of tomato fruit ripening [J]. Biosystems Engineering, 2009, 103(1): 116-119.

[19] Fracarolli J A, Enes A M, Dal Fabbro I M, *et al*. Laser transmission through vegetative material [J]. World Academy of Science Engineering and Technology, 2012, 6(10): 892-894.

[20] Mulone C, Budini N, Vincitorio F M, *et al*. Biospeckle activity evolution of strawberries[J]. SOP Transactions on Applied Physics, 2014, 1(2): 65-73.

[21] Pajuelo M, Baldwin G, Rabal H, *et al*. Bio-speckle assessment of bruising in fruits [J]. Optics and Lasers in Engineering, 2003, 40(1/2): 13-24.

[22] Kumari S, Nirala A K. Biospeckle technique for the non-destructive differentiation of bruised and fresh regions of an Indian apple using intensity-based algorithms [J]. Laser Physics, 2016, 26(11): 115601.

[23] Samuel B, Retheesh R, Ansari M Z, *et al*. Cross-correlation and time history analysis of laser dynamic specklegram imaging for quality evaluation and assessment of certain seasonal fruits and vegetables [J]. Laser Physics, 2017, 27(10): 105601.

[24] Samuel B, R R, Nampoori V P N, *et al*. Nondestructive evaluation of fruits using cross correlation and time history of biospeckle pattern[C] // Proceedings of 2016 National Seminar and International Exhibition on Nondestructive Evaluation, 2016: 470-473.

[25] Vega F, Torres M C. Automatic detection of bruises in fruit using biospeckle techniques[C] // Symposium of Signals, Images and Artificial Vision, 2013, 978: 1-5.

[26] Yan L, Liu J X, Men S. The biospeckle method for early damage detection of fruits[J]. Modern Physics Letters B, 2017, 31(19/20/21): 1740034.

[27] Liu H B, Gao Y W, Lu J Z, *et al*. Pear defect and stem/calyx discrimination using laser speckle [J]. Transactions of the Chinese Society of Agricultural Engineering, 2015, 31(4): 319-324.
刘海彬, 高迎旺, 卢劲竹, 等. 基于激光散斑的梨缺陷与果梗/花萼的识别[J]. 农业工程学报, 2015, 31(4): 319-324.

[28] Retheesh R, Ansari M Z, Radhakrishnan P, *et al*. Application of qualitative biospeckle methods for the identification of scar region in a green orange [J]. Modern Physics Letters B, 2018, 32(9): 1850113.

[29] Mulone C, Budini N, Vincitorio F M, *et al*. Analysis of strawberry ripening by dynamic speckle measurements [J]. Proceedings of SPIE, 2013, 8785: 87851X.

[30] Hashim N, Janius R, Baranyai L, *et al*. Application of RGB and backscattering imaging to detect chilling injury symptoms in banana[C] // CIGR Workshop on Image Analysis in Agriculture, Budapest. 2010: 66-78.

[31] Hashim N, Janius R B, Rahman R A, *et al*. Changes of backscattering parameters during chilling injury in bananas[J]. Journal of Engineering Science and Technology, 2014, 9(3): 314-325.

[32] Arefi A, Moghaddam P A, Hassanpour A, *et al*. Non-destructive identification of mealy apples using biospeckle imaging [J]. Postharvest Biology and Technology, 2016, 112: 266-276.

[33] Arefi A, Moghaddam P A, Motlagh A M, *et al*. Towards real-time speckle image processing for mealiness assessment in apple fruit[J]. International Journal of Food Properties, 2017, 20(Sup 3): S3135-S3148.

[34] Szymanska-Chargot M, Adamiak A, Zdunek A. Pre-harvest monitoring of apple fruits development with the use of biospeckle method [J]. Scientia Horticulturae, 2012, 145: 23-28.

[35] Pieczywek P M, Cybulska J, Szymańska-Chargot M, *et al*. Early detection of fungal infection of stored apple fruit with optical sensors: comparison of biospeckle, hyperspectral imaging and chlorophyll fluorescence[J]. Food Control, 2018, 85: 327-338.

[36] Romano G, Nagle M, Argyropoulos D, *et al*. Laser light backscattering to monitor moisture content, soluble solid content and hardness of apple tissue

during drying [J]. Journal of Food Engineering, 2011, 104(4): 657-662.

[37] Kurenda A, Pieczywek P M, Adamiak A, *et al*. Effect of cytochalasin B, lantrunculin B, colchicine, cycloheximid, dimethyl sulfoxide and ion channel inhibitors on biospeckle activity in apple tissue [J]. Food Biophysics, 2013, 8(4): 290-296.

[38] Kurenda A, Zdunek A, Schlüter O, *et al*. VIS/NIR spectroscopy, chlorophyll fluorescence, biospeckle and backscattering to evaluate changes in apples subjected to hydrostatic pressures [J]. Postharvest Biology and Technology, 2014, 96: 88-98.

[39] Pieczywek P M, Cybulska J, Zdunek A, *et al*. Exponentially smoothed Fujii index for online imaging of biospeckle spatial activity [J]. Computers and Electronics in Agriculture, 2017, 142: 70-78.

[40] Ansari M D Z, Nirala A K. Biospeckle activity measurement of Indian fruits using the methods of cross-correlation and inertia moments [J]. Optik, 2013, 124(15): 2180-2186.

[41] Ansari M Z, Minz P D, Nirala A K. Fruit quality evaluation using biospeckle techniques [C] // 2012 1st International Conference on Recent Advances in Information Technology (RAIT), 2012: 873-876.

[42] Ansari M D Z, Nirala A K. Biospeckle techniques in quality evaluation of indian fruits [J]. World Academy of Science, Engineering and Technology, 2012, 6(11): 978-982.

[43] Ansari M Z, Nirala A K. Assessment of bio-activity using the methods of inertia moment and absolute value of the differences [J]. Optik, 2013, 124(6): 512-516.

[44] Ansari M Z, Nirala A K. Assessment of fruits during shelf-life storage using biospeckle laser [J]. Agricultural Engineering International: CIGR Journal, 2014, 16(3): 223-229.

[45] Minz P D, Nirala A K. Assessment of bio-activity of the fruits using intensity based methods [C] // 2013 International Conference on Microwave and Photonics (ICMAP), 2013: 1-4.

[46] Peixoto L S, Fracarolli J A, Aguiar R H. Evaluation of minimally processed apples with application of edible films through biospeckle [J]. Journal of Agricultural Science and Technology B, 2016, 6(3): 201-208.

[47] Jamshidi B, Arefi A. Comparison of different feature extraction techniques in biospeckle images for nondestructive assessment of apple firmness [C] // Proceedings of the 3rd Iranian International NDT Conference, 2016.

[48] Nassif R, Nader C A, Afif C, *et al*. Detection of Golden apples' climacteric peak by laser biospeckle measurements [J]. Applied Optics, 2014, 53(35): 8276-8282.

[49] Nassif R, Pellen F, Magné C, *et al*. Scattering through fruits during ripening: laser speckle technique correlated to biochemical and fluorescence measurements [J]. Optics Express, 2012, 20(21): 23887-23897.

[50] Nassif R, Pellen F, Magne C, *et al*. Laser speckle dynamic for monitoring fruits maturation [J]. Proceedings of SPIE, 2012, 8413: 84131G.

[51] Affeldt H A, Heck R D. Optics for produce quality evaluation: laser diffusion for orange peel thickness measurement [J]. Proceedings of SPIE, 1993, 1836: 252-261.

[52] Bergkvist A. Biospeckle-based study of the line profile of light scattered in strawberries [J]. Lund Reports in Atomic Physics, 1997.

[53] Hashim N, Adebayo S E, Abdan K, *et al*. Comparative study of transform-based image texture analysis for the evaluation of banana quality using an optical backscattering system [J]. Postharvest Biology and Technology, 2018, 135: 38-50.

[54] Kalaj Y R, Geyer M, Herppich W B. Non-destructive evaluation of edible coatings effects on keeping quality of European plums (Prunus domestica L.) by laser light backscattering imaging [J]. Erwerbs-Obstbau, 2018, 60(4): 311-320.

[55] Kalaj Y R, Mollazade K, Herppich W, *et al*. Changes of backscattering imaging parameter during plum fruit development on the tree and during storage [J]. Scientia Horticulturae, 2016, 202: 63-69.

[56] Mohd Ali M, Hashim N, Bejo S K, *et al*. Laser-induced backscattering imaging for classification of seeded and seedless watermelons [J]. Computers and Electronics in Agriculture, 2017, 140: 311-316.

[57] Udomkun P, Nagle M, Mahayothee B, *et al*. Laser-based imaging system for non-invasive monitoring of quality changes of papaya during drying [J]. Food Control, 2014, 42: 225-233.

[58] Marcondes M S, Silva K G, Fujii A K, *et al*. Sugar cane (Saccharum officinarum L.) analysis through biospeckle and spectroscopy (NIR) [J]. Journal of Agricultural Science and Technology B, 2017, 7(1): 62-68.

[59] Ansari M Z, Nirala A K. Assessment of biospeckle activity of lemon fruit[J]. Agricultural Engineering International: CIGR Journal, 2016, 18(2): 190-200.

[60] Baranyai L, Zude M. Analysis of laser light propagation in kiwifruit using backscattering imaging and Monte Carlo simulation[J]. Computers and Electronics in Agriculture, 2009, 69(1): 33-39.

[61] Amaral I C, de Resende J V, Braga Jr R A, *et al*. Evaluation of the adsorption behavior of freeze-dried passion fruit pulp with added carriers by traditional biospeckle laser techniques[J]. Drying Technology, 2017, 35(1): 55-65.

[62] Zhu N, Lin M, Nie Y, et al. Study on the quantitative measurement of firmness distribution maps at the pixel level inside peach pulp[J]. Computers and Electronics in Agriculture, 2016, 130: 48-56.

[63] Duan Y T, Li G Y, Gao Z. Review of laser biospeckle measurement technology[J]. Laser & Optoelectronics Progress, 2013, 50(2): 17-29.
段怡婷, 李光宇, 高瞻. 生物散斑测量技术综述[J]. 激光与光电子学进展, 2013, 50(2): 17-29.

[64] Shi B Y, Bi K, Chen S H, *et al*. Application of laser speckle technology on the detection of agricultural products[J]. Chinese Agricultural Science Bulletin, 2011, 27(2): 410-415.
石本义, 毕昆, 陈四海, 等. 激光散斑技术在农产品检测中的应用[J]. 中国农学通报, 2011, 27(2): 410-415.

[65] Minz P D, Nirala A K. Bio-activity assessment of fruits using Generalized Difference and Parameterized Fujii method[J]. Optik, 2014, 125(1): 314-317.

[66] Cheng H Y, Luo Q M, Zeng S Q, *et al*. Modified laser speckle imaging method with improved spatial resolution[J]. Journal of Biomedical Optics, 2003, 8(3): 559-564.

[67] Liu Q. Laser speckle contrast imaging and its biomedical applications[D]. Wuhan: Huazhong University of Science and Technology, 2005.
刘谦. 激光散斑衬比成像技术及其应用的研究[D]. 武汉: 华中科技大学, 2005.

[68] Qiu J J, Zhang H Y, Luo W H, *et al*. Impact of averaged image speckle size on laser speckle imaging[J]. Acta Optica Sinica, 2009, 29(7): 1863-1867.
邱建军, 张红艳, 骆卫华, 等. 像面散斑平均尺寸对激光散斑成像的影响[J]. 光学学报, 2009, 29(7): 1863-1867.

[69] Zhang M J, Wang YH, Zhao G F, *et al*. Climate change during winter wheat growing period and its impacts on winter wheat yield in Puyang of Henen province[J]. Chinese Journal of Agrometeorology, 2009, 30(2): 223-229.
张明捷, 王运行, 赵桂芳, 等. 濮阳冬小麦生育期气候变化及其对小麦产量的影响[J]. 中国农业气象, 2009, 30(2): 223-229.

[70] Cai J R, Liu M L, Sun L, *et al*. Laser speckle image detection of chilled pork freshness based on improved moment of inertia algorithm[J]. Transactions of the Chinese Society of Agricultural Engineering, 2017, 33(7): 268-274.
蔡健荣, 刘梦雷, 孙力, 等. 基于改进惯性矩算法的冷鲜猪肉新鲜度激光散斑图像检测[J]. 农业工程学报, 2017, 33(7): 268-274.

[71] Minz P D, Nirala A K. Intensity based algorithms for biospeckle analysis[J]. Optik, 2014, 125(14): 3633-3636.

[72] Ansari M Z, Nirala A K. Biospeckle numerical assessment followed by speckle quality tests[J]. Optik, 2016, 127(15): 5825-5833.

[73] Cariñe J, Guzmán R, Torres-Ruiz F A. Algorithm for dynamic Speckle pattern processing[J]. Optics and Lasers in Engineering, 2016, 82: 56-61.